2010

Mzm1 Influences a Labile Pool of Mitochondrial Zinc Important for Respiratory Function

Aaron Atkinson
University of Utah Health Sciences

Oleh Khalimonchuk
University of Nebraska-Lincoln, okhalimonchuk2@unl.edu

Pamela Smith
University of Utah Health Sciences Center

Hana Sabic
University of Utah Health Sciences Center

David Eide
University of Wisconsin-Madison

See next page for additional authors

THE JOURNAL OF BIOLOGICAL CHEMISTRY VOL. 285, NO. 25, pp. 19450–19459, June 18, 2010

Mzm1 Influences a Labile Pool of Mitochondrial Zinc Important for Respiratory Function*

Received for publication, February 1, 2010, and in revised form, April 6, 2010 Published, JBC Papers in Press, April 19, 2010, DOI 10.1074/jbc.M110.109793

Aaron Atkinson[‡1], **Oleh Khalimonchuk**[‡], **Pamela Smith**[‡1], **Hana Sabic**[‡], **David Eide**[§], **and Dennis R. Winge**[‡2]

From the [‡]*Departments of Medicine and Biochemistry, University of Utah Health Sciences Center, Salt Lake City, Utah 84132 and the* [§]*Department of Nutritional Sciences, University of Wisconsin-Madison, Madison, Wisconsin 53706*

Zinc is essential for function of mitochondria as a cofactor for several matrix zinc metalloproteins. We demonstrate that a labile cationic zinc component of low molecular mass exists in the yeast mitochondrial matrix. This zinc pool is homeostatically regulated in response to the cellular zinc status. This pool of zinc is functionally important because matrix targeting of a cytosolic zinc-binding protein reduces the level of labile zinc and interferes with mitochondrial respiratory function. We identified a series of proteins that modulate the matrix zinc pool, one of which is a novel conserved mitochondrial protein designated Mzm1. Mutant *mzm1*Δ cells have reduced total and labile mitochondrial zinc, and these cells are hypersensitive to perturbations of the labile pool. In addition, *mzm1*Δ cells have a destabilized cytochrome *c* reductase (Complex III) without any effects on Complexes IV or V. Thus, we have established that a link exists between Complex III integrity and the labile mitochondrial zinc pool.

All known mitochondrial zinc-requiring metalloproteins are synthesized in the cytoplasm and must be imported as newly synthesized polypeptides into the organelle as with most resident proteins. Protein import into the mitochondria requires unfolded polypeptides, so folding and metallation occur upon import. Thus, a bioavailable pool of Zn(II) must be maintained within the mitochondria for efficient metallation reactions. The folding of metalloproteins is dependent on the availability and the selective insertion of the appropriate metal ion. Mis-metallation by a non-native metal ion may be deleterious yielding either an inactive protein or a misfolded state prone to aggregation.

The zinc mitochondrial metalloproteome is large relative to other metals and distributed throughout the organelle (1). The zinc proteome is heavily populated by proteases and in yeast include the iAAA, mAAA, Oma1, Oct1, Icp55, Atp23, and the MPP protease complex. These proteases all share an essential H*EXX*H or H*XX*EH metal-binding motif and whereas many metalloproteinases can be activated *in vitro* by diverse divalent cations, Zn(II) is likely to be the physiological metal ion bound.

Zn(II) is an abundant cofactor for a variety of additional metalloenzymes in mitochondria, including Adh3, Adh4, and Leu9 in the matrix, in addition to Cu,Zn Sod1 and Hot13 in the IMS (2). Last, cytochrome *c* oxidase requires Zn(II) in its Cox4 subunit (3).

Cellular Zn(II) acquisition in eukaryotes is achieved through a conserved ZIP (or SLC39) family of transporters (4). ZIP transporters in yeast (Zrt1 and Zrt2) and mammals predominately translocate Zn(II) from the extracellular space or organelles into the cytoplasm. A second class of eukaryotic Zn(II) transporters is the cation diffusion facilitator (CDF, ZnT, or SLC30) family that typically translocate Zn(II) from the cytoplasm either into organelles or out of the cell (4, 5). Both families of transporters are polytopic intrinsic membrane proteins. Fourteen candidate ZIP and ten distinct ZnT transporters are known in the human genome, whereas yeast possess five ZIP and five CDF transporters (6). Zn(II) transporters have been identified that mediate Zn(II) uptake into the ER, Golgi, and vacuole compartments (4), although no ZnT or ZIP mitochondrial transporters have been identified.

Within eukaryotic cells, labile Zn(II) pools have been identified using Zn(II)-responsive fluorophores (7, 8). Punctate fluorescent components seen in a myriad of cell types have been termed zincosomes (9), although the compartment has not been fully defined (4). Labile Zn(II) pools have been described in the brain, pancreas, prostate, and the retina. The correlation of the cellular fluorescence with labile Zn(II) pools is complicated by caveats such as the binding affinity of the fluorophore, discrimination among diverse metal ions, and a tendency of fluorophores to compartmentalize. Nonetheless, the visualization of labile Zn(II) pools with fluorophores of varying Zn(II) binding affinities suggests that cells contain pools of kinetically labile, ligand-bound Zn(II) (9).

One defined labile Zn(II) pool resides in presynaptic boutons in mossy fiber neurons within the hippocampus (7). These presynaptic vesicles are also enriched with glutamate as a neurotransmitter. The vesicles accumulate Zn(II) to ~0.3 mM through the ZnT-3 Zn(II) transporter (10–12). Synaptic cleft Zn(II) is a modulator of glutamate receptors and post-synaptic neuronal Zn(II) may have a second messenger effect.

Labile Zn(II) is also seen in secretory granules in pancreatic β cells, mast cells, intestinal paneth cells, and prostate epithelial cells (8). Ligands stabilizing the labile Zn(II) pools have not been defined, although the presence of high citrate in prostate secretory granules and glutamate in mossy fiber neuronal granules suggest that these compounds may stabilize Zn(II).

Labile Zn(II) pools have also been observed within mitochondria. A labile mitochondrial Zn(II) pool distinct from protein-bound Zn(II) was identified using the mitochondrial-spe-

* This work was supported, in whole or in part, by National Institutes of Health Grants GM083292 (to D. R. W.) and GM56285 (to D. E.).
[1] Supported by National Institutes of Health Training Grant T32 DK007115.
[2] To whom correspondence should be addressed: University of Utah Health Sciences Center, Salt Lake City, UT 84132. Tel.: 801-585-5103; Fax: 801-585-5469; E-mail: dennis.winge@hsc.utah.edu.

cific Zn-responsive fluorophore RhodZin-3 in neuronal cells (13, 14). The labile pool was shown to be dependent on the IM membrane potential and to be mobilized upon mitochondrial depolarization. No information exists on the ligands that stabilize labile Zn(II) in mitochondria nor the effects of zinc status on this pool.

We describe presently the identification of a labile Zn(II) pool within yeast mitochondria that is responsive to the exogenous Zn(II) level. High throughput screens were conducted to identify proteins important for the maintenance of the mitochondrial labile Zn(II) pool. One protein identified, Mzm1, was found to be important for both the maintenance of matrix zinc and assembly/stability of the respiratory Complex III. These studies establish a link between Complex III and mitochondrial zinc pools.

MATERIALS AND METHODS

Yeast Strains and Media—BY4741 and BY4743 strains deleted for *mzm1*Δ, *cit1*Δ, *mis1*Δ, *mdh1*Δ, *msb1*Δ, *nfu1*Δ, *and tbs1*Δ were purchased from Invitrogen and verified with open-reading frame (ORF)[3]-specific PCR primers. Disruption of *MZM1* in the W303 background was accomplished by substituting the *Candida albicans URA3* coding sequence. A 13Myc epitope was fused to the 3′ of the chromosomal-encoded MZM1 ORF (Mzm1-Myc) in the W303 background. EDTA supplementation (1 mM final concentration) to liquid synthetic complete medium was used to limit Zn availability for wild-type cells. Lower levels of EDTA were used with mutant strains when necessary. Strains were subsequently grown by serial dilutions on plates with EDTA supplementation adjusted as needed between 50 and 300 μM. For large scale m-Adh1 limitation of mitochondrial zinc, cells were grown in glassware washed with acid (5% nitric acid, 1% HCl) using culture medium made with yeast nitrogen base lacking Zn salts. For the EDTA-based robotic screen, 0.2–0.5 mM EDTA supplementation was added to non-fermentable glycerol medium. Standard synthetic complete medium was used in all other screens.

Expression Vectors—A pVT102-based Adh1::HA expression clone (herein referred to as c-Adh1) utilizing the minimal, non-zinc regulated *ADH1* promoter was constructed by Dr. Amanda Bird. To target c-Adh1 to the mitochondrial matrix, the targeting sequence from Sod2 was fused to the *ADH1* ORF using mega-primer PCR and gap-repair, herein referred to as m-Adh1. Similarly the catalytically inactive m-Adh1 was generated by an alanine substitution of a critical threonine at position 48 (15) by overlap extension PCR.

Robotic Screen—A collection consisting of deletion strains of 684 nuclear-encoded genes whose products were identified in a survey of the yeast mitochondrial proteome was arrayed in a 96-well format. Growth was tested using robotically applied serial dilutions of the strains on non-fermentable medium supplemented with 0.4 mM EDTA. Similarly, the strain collection was transformed with m-Adh1 (T48A) and screened for candidates showing m-Adh1-dependent growth inhibition on non-fermentable medium.

[3] The abbreviations used are: ORF, open-reading frame; ICP, inductively coupled plasma; BN, blue native; HA, hemagglutinin; WT, wild type.

Preparation of Mitochondria—Mitochondria were isolated as described previously (16). Briefly, lyticase was used to create spheroplasts that were subsequently ruptured by vortexing with glass beads or Dounce homogenizing for protein localization experiments. Intact mitochondria were purified from the cellular lysate using differential centrifugation and a discontinuous Nycodenz gradient (14 and 22%). Mitochondria were then centrifuged at 12,000 × *g* to concentrate before analysis. Protein concentrations were determined using standard Bradford protein reagents.

Mitochondrial Fractionation—To isolate submitochondrial fractions, the outer membrane was lysed in 10 mM Tris-HCl, pH 7.4 (or 20 mM HEPES, pH 7.2 for protein localization experiments), and the lysate subsequently centrifuged at 25,000 × *g* to separate the soluble IMS contents from mitoplasts retaining matrix contents in the pellet fraction. To isolate soluble matrix contents, mitoplasts were sonicated and again centrifuged at 25,000 × *g* to separate soluble matrix contents from the membrane fraction in the pellet. For batch-binding experiments, either hydrated carboxymethyl cellulose 52 (CM-52) or DEAE-52 ion exchange resins (Whatman) were added to soluble mitochondrial lysate at 4 °C with elution in 1 M ammonium acetate, pH 7.4, when needed. For fractionation of mitochondrial Zn, whole mitochondria were lysed by sonication in buffer A (20 mM ammonium acetate pH 7.4) using three 30-s pulses of sonication at 70% output of a microtip. The soluble fraction was then isolated by centrifugation at 15,000 × *g*. The soluble fraction was further diluted into buffer A, filtered through a 0.45 μM filter and injected onto either pre-equilibrated HR5/5 MonoQ or MonoS columns. The unbound fractions were washed off with 5 column volumes of buffer A. A 25–35 column-volume gradient of buffer B (1 M ammonium acetate, pH 7.4) was then initiated. Treatments of mitochondrial Zn samples, or free zinc controls were as follows: soluble mitochondrial lysate was boiled for 5 min and clarified by centrifugation 15,000 × *g* prior to injection; for citrate competition experiments, a 10-fold excess of citrate was mixed with either a MonoS-prepurified Zn-ligand sample or buffered free Zn and immediately injected onto MonoS and fractionated as above. For size exclusion chromatography, concentrated cationic fractions were injected on a Sephadex G-25 column pre-equilibrated in 2× phosphate-buffered saline. Fractions were collected and analyzed either by atomic absorption or inductively coupled plasma (ICP) spectroscopy.

Western Blot and Blue Native (BN) PAGE Analysis—For Western blot analysis, 20–50 μg of total protein from mitochondria was separated on a 12% SDS-PAGE gel system and transferred onto nitrocellulose membranes for analysis. Membranes were blocked prior to detection using 10% nonfat dry milk in 1× PBS (50 mM Na_2PO_4, 100 mM $NaCl_2$), and 0.01% Tween 20. BN-PAGE was done essentially as described previously (17) with either 1% digitonin or 1% dodecylmaltoside used to solubilize samples. Blots were reprobed after stripping in 3–5 washes of 25 mM glycine pH 2.0, 100 mM $NaCl_2$, and 0.5% Tween 20. Antibodies to porin (Por1), hemagglutinin (HA), phosphoglycerate kinase 1 (Pgk1) were obtained from Molecular Probes. Cox1, Cox2, and Cox3 antibodies were purchased from Mitosciences. Antisera to mitochondrial aconitase (Aco1)

was a gift from Dr. J. Kaplan. Antisera to the Rieske iron sulfur protein (Rip1) was a gift from Dr. B. Trumpower. Antisera to cytochrome 1 (Cyt1) was a gift from Dr. B. Meunier. Antisera to cytochrome b_2 was provided by Dr. C. Koehler. Anitsera to the F1 ATPase beta subunit (Atp2) and core protein 2 (Cor2) were provided by Dr. A. Tzagoloff.

Metal Analysis—For ICP-OES mitochondria, were resuspended in 200 μl of metal-free 40% nitric acid (Optima) and heated to 95 °C for 2 min. Soluble fractions were read directly after dilution with 10% nitric acid. Volumetric serial dilutions of commercially available mixed metal standards were used to generate standard curves. For Atomic Absorption Spectroscopy, soluble fractions were compared with suitable blank readings and concentrations calculated from ICP-verified standards. The Zn-dependent fluorophore, RhodZin-3 dipotassium salt (Molecular Probes) was used to assess labile zinc concentrations. Either submitochondrial fractions, or soluble mitochondrial contents from 20–100 μg of total mitochondria sonicated in cold 10 mM Tris, pH 7.4, were analyzed in triplicate. Samples were diluted 1:5 in cold 30–60 μM RhodZin-3, 10 mM Tris, pH 7.4, and allowed to incubate for 30 s prior to measuring maximal emission at 575 nm (excitation at 535 nm) on a Perkin Elmer SS55 fluorimeter.

Measurement of Mitochondrial Respiration—Oxygen consumption by cells grown to stationary phase and then diluted to an A_{600} of 0.5 in 3 ml of 5% glycerol was determined using a 5300A biological oxygen monitor (Yellow Springs Instrument Co.). Activities of the respiratory complexes were measured as previously reported using 10–20 μg of mitochondria in 40 mM KH_2PO_4 pH 6.7, 0.5% Tween 20 with 32 μM horse cytochrome *c* (18). Cytochrome *c* was chemically reduced using sodium hydrosulfite for Complex IV activities; to measure the coupled Complex II/III activity cytochrome *c* reduction was monitored upon succinate addition in the presence of KCN to inhibit Complex IV. For Complex III measurements, the reduction of bovine cytochrome *c* was measured using the same buffer system and KCN inhibition as above. Complex III was directly reduced by 20 μM of the reduced ubiquinone analog, decylubiquinone (Sigma). Reduced decylubiquinone was prepared anaerobically using saturated sodium borohydride. Excess borohydride was later reacted with 6 N HCl while venting to allow release of hydrogen gas. Any precipitates in the reduced decylubiquinone were spun down and the solution transferred to a fresh vial under nitrogen. The decylubiquinone concentration was determined on a pre-reduced aliquot using the molar extinction coefficient (ϵ) of 12.5 mM^{-1} cm^{-1} at 275 nM.

RESULTS

Distribution of Zn within Mitochondria—The zinc content of gradient-purified mitochondria was assessed in cells cultured in YPD (1% dextrose) medium in the presence and absence of supplemental $ZnCl_2$. The Zn content was found to be maintained at a nearly constant value until supplemental zinc levels exceeded 200 μM, at which point an expansion in mitochondrial zinc content was observed (Fig. 1*A*). To assess the distribution of zinc within mitochondria, purified and sonicated mitochondria were fractionated into soluble and particulate (pellet) fractions and subjected to ICP-OES analysis. As can be seen in Fig. 1*B*, Zn(II) was equally distributed between these fractions in mitochondria from cells cultured in unsupplemented YPD medium. Mitochondria from cells supplemented with 200 μM Zn(II) contain a 3-fold expansion of total zinc that was also equally distributed between soluble and particulate fractions. The soluble fractions from Zn-supplemented and unsupplemented cells were further fractionated by adsorption to DEAE- or CM-cellulose to isolate their cationic and anionic components, respectively. Zn(II) was similarly distributed between cationic and anionic pools in mitochondria from zinc-supplemented and unsupplemented cells. Cationic and anionic Zn(II) fractions obtained from unsupplemented cultures were incubated with the Zn-responsive RhodZin-3 fluorophore (Fig. 1*C*). The fluorescence of the cationic Zn fraction significantly exceeded that of the anionic Zn fraction despite having a similar zinc concentration suggesting that the cationic Zn fraction possessed greater kinetic reactivity.

The soluble mitochondrial lysates isolated from control and Zn-supplemented cells were adsorbed to MonoS and MonoQ ion exchange resins to further fractionate the cationic and anionic pools, respectively (Fig. 1, *D* and *F*). MonoS and MonoQ columns were eluted with a gradient of ammonium acetate. A major Zn-containing fraction was observed in the eluate of each exchanger, and the abundance of each component was increased in mitochondria isolated from Zn-supplemented cells. To assess the nature of the Zn component in the eluate of each exchanger, the mitochondrial lysate isolated from Zn-supplemented cells was first pretreated by boiling prior to the chromatography. Whereas the Zn component in the MonoQ eluate was depleted by boiling, the Zn component in the MonoS eluate was largely stable (Fig. 1, *D* and *F*). The MonoS Zn component was also resistant to proteinase K digestion suggesting that the MonoS Zn component is not protein bound (data not shown). To determine whether this cationic Zn component represents unbound Zn(II), both $ZnCl_2$ and the purified cationic Zn complex were incubated with citrate prior to MonoS chromatography. As shown in Fig. 1*E*, the elution position of the cationic Zn component was unchanged, whereas no Zn(II) was seen in the eluate during chromatography of a preformed Zn-citrate complex. The cationic Zn complex eluted from Sephadex G-25 near the internal volume consistent with a low mass Zn(II) complex (Fig. 1*G*). These data indicate that the cationic pool of labile zinc in the mitochondrial matrix is largely complexed with one or more compounds of low molecular mass. We will refer to this labile zinc pool as the cationic zinc pool because it adsorbs on cation exchangers and appears to be a monodisperse component.

Effect of a Heterologous Zn Competitor on Mitochondrial Zn Distribution—We previously demonstrated that the bioavailable Cu(I) pool in yeast mitochondria was titrated out by the presence of heterologous Cu(I)-binding proteins targeted to the mitochondrial matrix (19, 20). To determine whether a similar situation existed with the mitochondrial Zn fractions, we fused the Sod2 mitochondrial targeting sequence (MTS) to the cytoplasmic Adh1 molecule, designated m-Adh1, resulting in mitochondrial localization (Fig. 2*A*). Two m-Adh1 constructs were engineered. One fusion was the WT Adh1 sequence, whereas the second fusion was a catalytically inactive Adh1 allele (T48A). Yeast containing the

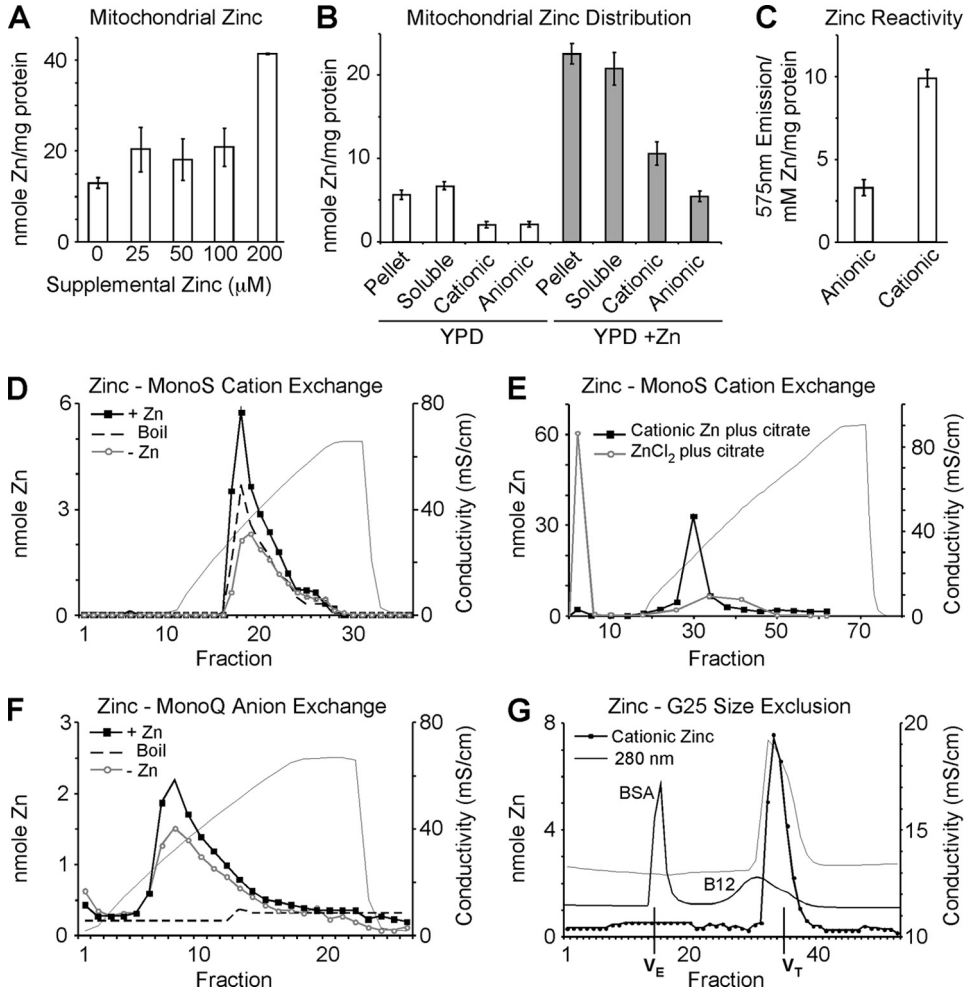

FIGURE 1. **Mitochondrial zinc pools.** Yeast cultures were grown in yeast peptone 1% dextrose (YP1D) medium and supplemented with 0–200 μM $ZnCl_2$. Mitochondria were isolated from cultures in triplicate and analyzed for zinc either from total or submitochondrial fractions by ICP-OES. *Panel A*, titration of supplemental zinc to cell cultures results in expansion of mitochondrial zinc. *Panel B*, soluble and pellet fractions were isolated from 0.5 mg of mitochondria by sonication and centrifugation. Ion exchange using either CM-52 or DEAE-52 cellulose was used to separate cationic and anionic fractions respectively. *Panel C*, using the Zn-dependent fluorophore Rhodzin-3, reactive zinc was assessed in mitochondrial lysate from 0.1 mg of mitochondria depleted of either anionic or cationic Zn pools (post DEAE-52 or CM-52 binding, respectively; $n = 4$). *Panels D–F*, MonoS and MonoQ ion exchange chromatography. Mitochondria were isolated from YP1D yeast cultures grown with 0.2 mM Zn (+Zn) or without (−Zn, Endogenous) and samples (equivalent to 0.5 mg of protein) were sonicated, clarified, and boiled where indicated. *Panel D*, fractionation of soluble lysate using MonoS shows a single cationic zinc peak that expands in response to zinc supplementation and is resistant to boiling. *Panel E*, either free Zn(II) in the form of $ZnCl_2$ or previously purified mitochondrial cationic Zn were mixed with a 10-fold excess of citrate and examined for the ability to bind to MonoS cation exchange resin. *Panel F*, fractionation of soluble lysate using MonoQ anion exchange reveals a broad peak that expands modestly in response to zinc supplementation, yet is not resistant to boiling. *Panel G*, gel filtration of the cationic zinc fraction isolated by MonoS elutes on a G25 size exclusion column in a volume corresponding to salt. 280 nm absorbance for both bovine serum albumin (*BSA*) and Vitamin B12 (*B12*) are shown. Volume exclusion (V_E) and volume total (V_T) are marked.

m-Adh1 fusions as well as a control Adh1 construct lacking the MTS (c-Adh1) were plated on Zn-limiting growth medium containing either glucose or glycerol in order to assess the effects of the matrix targeted Adh1 (Fig. 2*B*). Cells harboring m-Adh1 and m-Adh1 (T48A) showed a growth impairment on glycerol/lactate medium and growth on this medium was enhanced by the inclusion of supplemental Zn(II) suggesting that the respiratory growth impairment was a Zn effect. To confirm the Zn effect, *zrt1*Δ cells lacking the high affinity Zn(II) permease Zrt1 were transformed with plasmids encoding either c-Adh1 or m-Adh1. The presence of m-Adh1 in *zrt1*Δ cells compromised respiratory growth without requiring zinc-limiting culture medium (Fig. 2*C*).

Mitochondria were purified from yeast transformants to assess mitochondrial zinc levels. Mitochondria isolated from m-Adh1 cells cultured in standard complete medium exhibited a marked increase in mitochondrial Zn (Fig. 2*D*) and chromatography of soluble lysates on MonoS revealed a comparable level of the cationic Zn component in the elution gradient, whereas elevated Zn(II) was detected in the column wash fractions. Treatment of the soluble lysate with RhodZin-3 revealed no change in fluorescence in lysates isolated from c-Adh1 mitochondria *versus* m-Adh1 mitochondria (Fig. 2*D*, *right panel*). Thus, the presence of m-Adh1 in the mitochondria of cells propagated on synthetic complete growth medium leads to an expansion of the mitochondrial zinc content to accommodate the high Adh1 levels. This is further evidence of homeostatic control of the mitochondrial zinc pool.

In contrast to the marked expansion of mitochondrial Zn seen in mitochondria isolated from m-Adh1 transformants cultured in standard growth medium, the use of Zn-limiting conditions (synthetic culture medium prepared from Zn-deficient nitrogen base) yielded mitochondria with a slight diminution in total mitochondrial Zn from m-Adh1-containing cells (Fig. 2*E*). MonoS chromatography of soluble lysates from these mitochondria revealed a decrease in the cationic Zn component and corresponding increase in the Zn content of the unabsorbed wash fractions that contained Adh1 immunoreactivity (data not shown). Mitochondrial lysates from either c-Adh1 or m-Adh1 cells were incubated with RhodZin-3 under conditions of equal total mitochondrial protein levels, and the lysates from m-Adh1 mitochondria showed a dramatic attenuation in RhodZin-3 reactivity. Thus, the presence of m-Adh1 led to a marked shift of the RhodZin-3 reactive cationic Zn pool to Zn associated with m-Adh1. These conditions correlate with the respiratory growth defect observed in Fig. 2*B*.

High-throughput Screen of Yeast Deletion Strains for Attenuation in Labile Mitochondrial Zn—To identify proteins important for maintenance of the labile zinc pool, we conducted two high-throughput screens of yeast deletion mutants affecting genes of known or predicted mitochondrial proteins. Of the 851

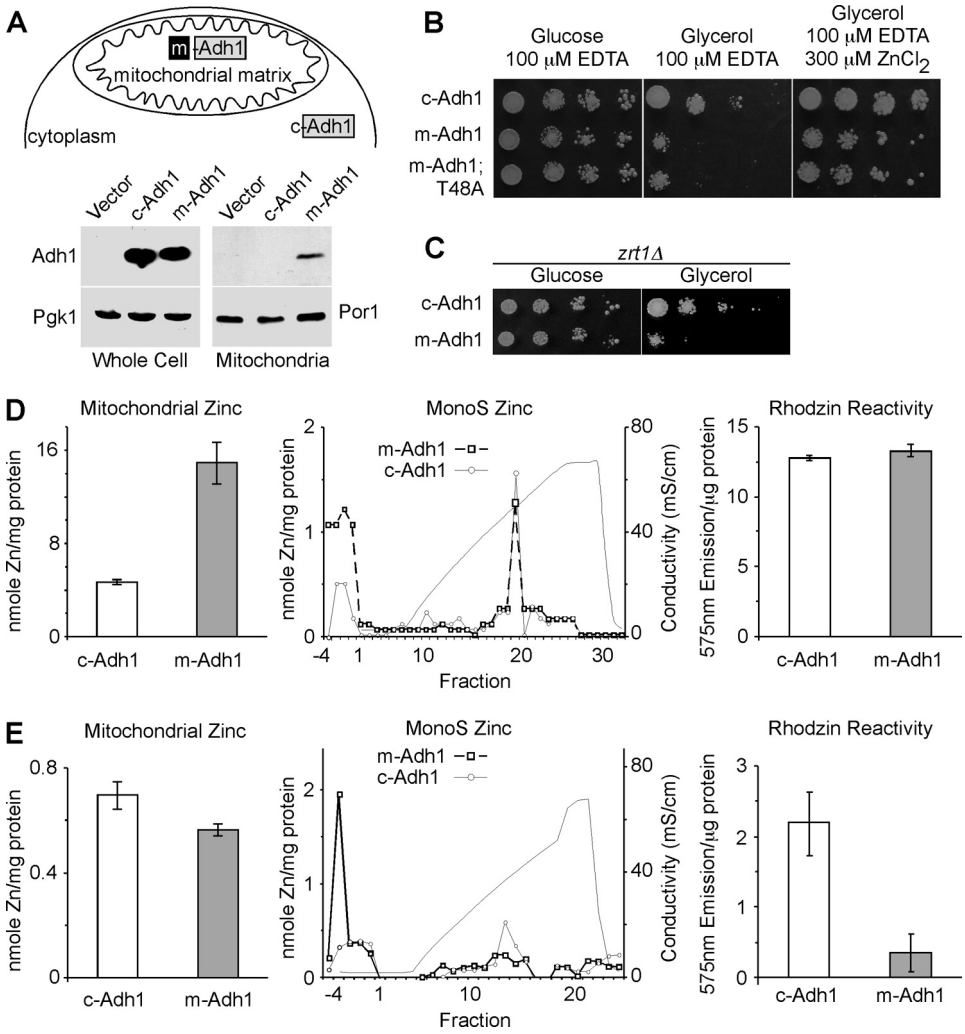

FIGURE 2. **Effect of matrix-targeted Adh1 (m-Adh1) on mitochondrial zinc.** *Upper panel A*, a schematic depicting the N-terminal fusion of the Sod2 mitochondrial targeting sequence directing Adh1 to the matrix, where upon import the Sod2 presequence is removed. *Lower panel A*, relative expression of c-Adh1 and m-Adh1 in both whole cell extracts and gradient-purified mitochondria relative to the respective loading controls Pgk1 and Por1. *Panel B*, wild-type yeast expressing either m-Adh1, or a catalytic inactive m-Adh1 mutant (T48A), show respiratory phenotypes when grown under Zn-limited conditions that are suppressed in the presence of excess Zn. *Panel C*, yeast lacking the plasma membrane zinc transporter, Zrt1, show an m-Adh1-induced respiratory phenotype without EDTA supplementation. *Left panel D*, total mitochondrial zinc from both c-Adh1- and m-Adh1-expressing cells obtained from cultures grown in synthetic complete Zn-replete medium. *Right panel D*, MonoS fractionation and Rhodzin-3 fluorescence ($n = 3$) of soluble mitochondrial lysates from either c-Adh1- or m-Adh1-expressing cultures. *Left panel E*, total mitochondrial zinc from both c-Adh1- and m-Adh1-expressing cells obtained from cultures grown in synthetic complete Zn-deficient medium. *Right panel E*, MonoS fractionation and Rhodzin-3 fluorescence ($n = 3$) of soluble mitochondrial lysates Zn-deficient cultures.

total proteins in the mitochondrial proteome identified to date, 684 are not essential for growth. These 684 viable mutant strains were arrayed in 96-well microtiter plates amenable to robotic manipulations.

Initially, serial dilutions of the strains were performed robotically and the cells were plated on Zn-limited culture medium (YP glycerol/lactate containing 0.4 mM EDTA). Ten deletion strains initially exhibited partial growth impairment on Zn-limited glycerol/lactate medium. Of these, only one strain (YDR493W renamed *mzm1*Δ, Mzm1 designating mitochondrial zinc maintenance) exhibited highly reproducible Zn-sensitive respiratory growth. The *mzm1*Δ strain exhibited a growth defect on glycerol/lactate medium when Zn(II) was limiting, and this phenotype was suppressed by zinc supplements. In addition, the *mzm1*Δ mutant grew poorly at 37 °C in the absence of Zn limitation. These effects were largely suppressed by introduction of the *MZM1* gene on a plasmid (Fig. 3*A*). However, growth of the mutant on glycerol/lactate medium at 37 °C was only partially restored by the addition of supplemental zinc salts indicating that exogenous zinc does not completely restore the cell to a normal state. Cells lacking Mzm1 also grew poorly when transformed with an episomal vector expressing m-Adh1 and cultured on glycerol/lactate medium (Fig. 3*B*). The growth impairment was observed only in cells containing m-Adh1 and not c-Adh1. Thus, *mzm1*Δ mutants grow poorly on respiratory carbon sources when zinc is limiting and this effect is reproduced by mitochondrial zinc depletion caused by m-Adh1 expression.

The second high throughput screen involved transforming the 684 deletion strains with a vector encoding the catalytically inactive T48A m-Adh1. Transformants were serially diluted and plated on glucose and glycerol/lactate culture medium. Thirty-five strains exhibiting a defect on glycerol/lactate only in the presence of m-Adh1 (T48A) were collected for subsequent analysis. Transformation was repeated with the 35 candidate deletion strains using both m-Adh1 and c-Adh1, and transformants were plated on medium in the presence and absence of supplemental zinc. In addition to *mzm1*Δ cells, we identified six other mutant strains that exhibited a reproducible growth impairment on glycerol/lactate medium in the presence of m-Adh1 but not c-Adh1 (Fig. 4*A*). These included *cit1*Δ, *mdh1*Δ, *mis1*Δ, *msb1*Δ, *nfu1*Δ, and *tbs1*Δ cells. Limited rescue of the growth defect of certain transformants was achieved by supplemental zinc. Mitochondria purified from the six deletion strains were used for quantitation of total mitochondrial zinc by ICP-OES analysis and labile zinc by RhodZin-3 reactivity. Mitochondrial zinc was depressed in the *cit1*Δ, *mdh1*Δ, and *tbs1*Δ cells and RhodZin-3 reactivity was also attenuated in these strains with an especially marked reduction in *mdh1*Δ cells (Fig. 4*B*). Cit1 and Mdh1 are the citric acid cycle enzymes citrate synthase and malate dehydrogenase, whereas Tbs1 is a large 1095-residue mitochondrial protein of

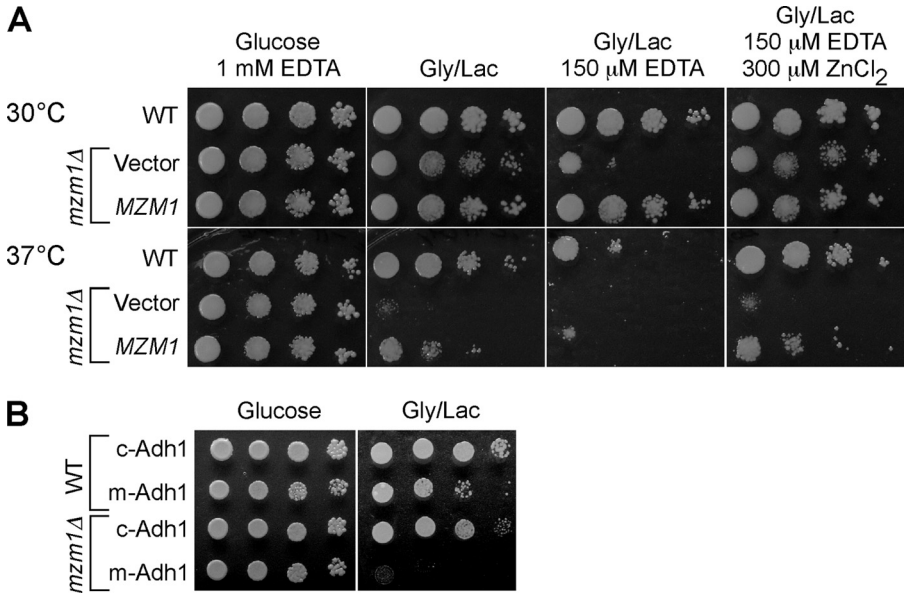

FIGURE 3. **Zn-dependent respiratory defects.** In a large-scale screen for mutants showing Zn-dependent respiratory defects, we isolated *mzm1*Δ from a collection of 684 deletion strains lacking proteins predicted to have mitochondrial localization. *Panel A*, *mzm1*Δ cells are unable to grow on respiratory carbon sources under Zn-limited conditions (EDTA) or at elevated temperature relative to both wild type and the complemented strain. *Panel B*, the presence of m-Adh1 severely restricts *mzm1*Δ respiratory growth.

unknown function. The marked respiratory defect of *mzm1*Δ mutants in zinc-limited medium and that it was an un-annotated ORF led us to focus our subsequent studies on the characterization of Mzm1.

Mzm1 Is Localized within the Mitochondrial Matrix—Mzm1 is a 13.9-kDa mitochondrial protein (21). The chromosomal *MZM1* was epitope tagged with Myc to generate a C-terminal Myc-tagged protein. The tagged protein is functional and retained in mitoplasts and was resistant to proteinase K in both intact mitochondria and mitoplasts (Fig. 5*A*). The Mzm1 protein was released by sonication of mitochondria suggesting it is a soluble matrix protein (Fig. 5*B*). The exclusive mitochondrial localization of Mzm1 was recently shown by an alpha complementation test (22). Mzm1 is not part of a large protein complex; the protein fractionates as a lower mass protein during sucrose gradient centrifugation (Fig. 5*C*).

*Mitochondrial Phenotypes of mzm1*Δ *Cells*—The growth phenotypes of *mzm1*Δ mutants suggest that zinc homeostasis in mitochondria is disrupted. Consistent with this hypothesis, mitochondria purified from *mzm1*Δ cells have decreased Zn content with no significant changes in iron, copper, manganese, or magnesium levels (Fig. 6*A*, data not shown). The mutant cells also show a marked decrease in RhodZin-3 reactivity consistent with a diminished cationic Zn component (Fig. 6*B*). This was corroborated by fractionation of mitochondrial lysates from WT *versus mzm1*Δ cells by ion exchange chromatography. The anionic Zn fraction was not perturbed in *mzm1*Δ cells (Fig. 6*D*), but the cationic Zn fraction was greatly reduced (Fig. 6*E*).

As mentioned, *mzm1*Δ cells are impaired for respiratory growth at 37 °C and at 30 °C upon zinc limitation. To assess the respiratory capacity of the mutant cells, oxygen consumption was measured in WT and mutant cells (Fig. 7*A*). Total oxygen consumption was reduced in the mutant cells at both 30 °C and 37 °C. Activities of Complexes III and IV were assessed in both W303 and BY4741 genetic backgrounds and the *mzm1*Δ cells were found to have a marked reduction in the activity of Complex III (bc_1) measured either as succinate cytochrome *c* reductase activity or ubiquinol cytochrome *c* reductase activity (Fig. 7*B*). Complex IV (cytochrome *c* oxidase) activity was unaffected in the *mzm1*Δ strain.

Impaired bc_1 Complex Activity Was Corroborated by Analysis of the Respiratory Complexes—Dodecyl maltoside solubilization reduces supercomplexes to individual complexes that can be separated by BN-PAGE. Visualization of the bc_1 complex using antibodies to three separate subunits revealed its attenuation in *mzm1*Δ cells (Fig. 8*A*, *lanes 2*, *4*, *6*). Despite disruption of the assembled bc_1 complex, the steady-state levels of bc_1 subunits Cyt1 and Cor2 were not changed (Fig. 8*B*). However, a partial decrease in steady-state levels of Rip1 was seen in *mzm1*Δ cells. Although the bc_1 complex abundance was diminished, no change was observed in either cytochrome *c* oxidase or ATP synthase complexes (Fig. 8*A*, *lanes 8* and *10*, respectively). As expected from the decrease in the bc_1 complex, the abundance of bc_1/cytochrome *c* oxidase supercomplexes was significantly reduced in *mzm1*Δ cells as observed with digitonin solubilization (Fig. 8*C*, *lanes 2* and *4*). No changes were evident in the monomeric and dimeric ATP synthase complexes (Complex V) (Fig. 8*C*, *lanes 5* and *6*). Because *mzm1*Δ cells show decreased matrix Zn(II), we tested whether zinc supplements would restore bc_1 activity. Mutant cells cultured in 200 μM Zn(II) failed to restore bc_1 activity (data not shown).

DISCUSSION

We demonstrate for the first time that a bioavailable pool of Zn(II) exists within the mitochondrial matrix that appears to be critical for mitochondrial function. This pool can be titrated out by expressing a matrix-targeted Zn-binding protein, m-Adh1, in cells propagated in Zn-limiting medium. The labile Zn(II) pool is ligand-bound and is cationic in nature. It is stable in the presence of citrate as a competitor but is reactive with the Zn-responsive fluorophore RhodZin-3. The matrix bioavailable Zn(II) pool increases in cells cultured with supplemental Zn(II) salts in excess of 200 μM. Current studies are underway to structurally characterize this cationic Zn component.

The physiological significance of the matrix Zn(II) pool may relate to either a detoxification mechanism for the metal or a Zn(II) reservoir for metallation of Zn-binding proteins within the matrix. Previous work demonstrated that the yeast vacuole is the major reservoir of excess Zn(II) accumulated in cells cultured in high zinc (23–25). A marked expansion of the mitochondrial matrix zinc pool does not occur when the medium

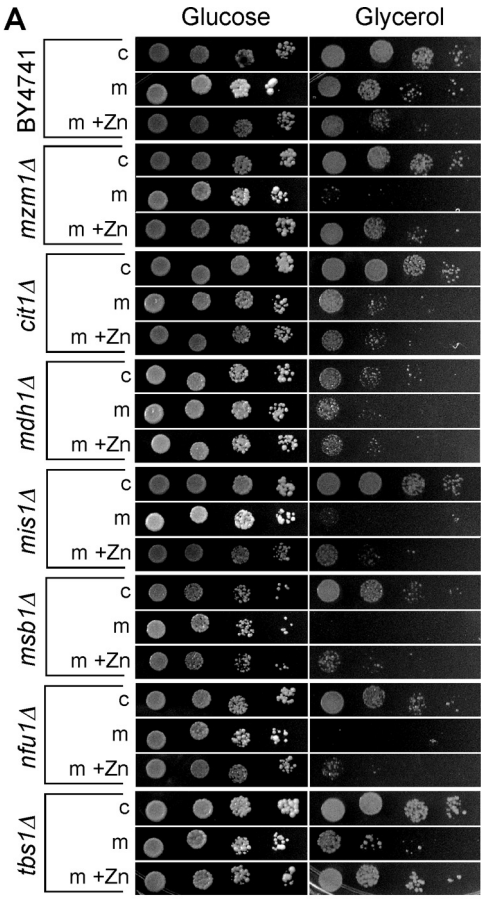

B

Genotype	Mitochondrial Zinc	Reactive Zinc
BY4741	1.95 ± 0.19	0.78 ± 0.05
*cit1*Δ	1.76 ± 0.08 (p<0.05)	0.55 ± 0.08 (p<0.05)
*mdh1*Δ	1.66 ± 0.29 (p<0.05)	0.12 ± 0.13 (p<0.05)
*mis1*Δ	2.09 ± 0.32	0.63 ± 0.07 (p<0.05)
*msb1*Δ	2.05 ± 0.31	0.59 ± 0.08 (p<0.05)
*nfu1*Δ	1.90 ± 0.14	0.69 ± 0.08
*tbs1*Δ	1.65 ± 0.17 (p<0.05)	0.40 ± 0.10 (p<0.05)
	(nM Zn/mg protein)	(575 Emission/ mM Zn/mg protein)

FIGURE 4. **m-Adh1-induced respiratory deficiency.** *Panel A*, yeast *mzm1*Δ, *cit1*Δ, *mdh1*Δ, *mis1*Δ, *msb1*Δ, *nfu1*Δ, and *tbs1*Δ strains were identified as m-Adh1 (T48A) sensitive from the collection of 684 strains lacking predicted mitochondrial proteins. Strains were re-transformed with either c-Adh1 or m-Adh1 (T48A) and grown in either synthetic complete (SC) glucose medium without (−Zn) or with (+Zn) 500 μM supplemental $ZnCl_2$. Cultures were then serially diluted onto SC medium agar with glucose or glycerol as carbon sources. All strains were verified by PCR using a universal KanMX and gene-specific primers. *Panel B*, mitochondria from *cit1*Δ, *mdh1*Δ, *mis1*Δ, *msb1*Δ, *nfu1*Δ, and *tbs1*Δ cells were purified from cells grown in standard SC 1% glucose medium for comparison to wild-type mitochondria. Both total mitochondrial zinc and reactive zinc, as assessed with Rhodzin-3, were measured in triplicate on three independent mitochondrial preparations.

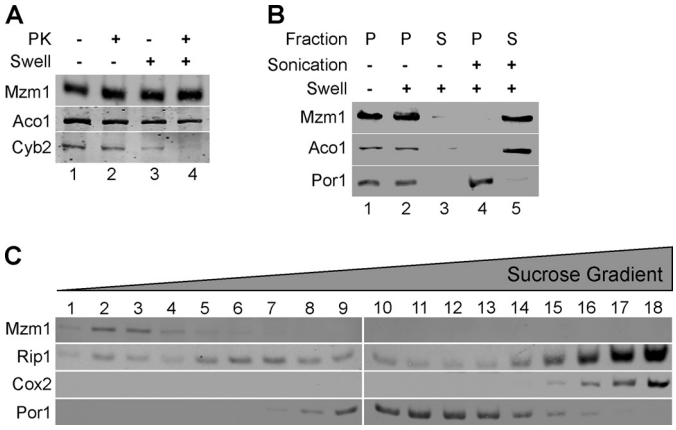

FIGURE 5. **Localization of Mzm1.** *Panel A*, mitochondria (100 μg) expressing Mzm1-Myc were kept intact (− swell, *lanes 1* and *2*) or swollen (+ swell, *lanes 3* and *4*) and incubated with (*lanes 2* and *4*) or without (*lanes 1* and *3*) proteinase K (PK). The matrix marker protein is Aco1, mitochondrial aconitase; inner mitochondrial space protein is Cyb2, cytochrome b_2. *Panel B*, mitochondria (100 μg of protein) were fractionated using both hypotonic lysis (swelling) and sonication. Pellet (*P*) and soluble (*S*) fractions were isolated by centrifugation (see "Materials and Methods" for details). In swollen mitoplasts in the absence of sonication, Mzm1 and Aco1 are retained in the pellet fraction. Detection with porin (Por1) antibody marks the pellet fraction. *Panel C*, mitochondria (1 mg) were solubilized in buffer containing 1% digitonin and centrifuged over a continuous 7–30% sucrose gradient. Mzm1-Myc migration is shown relative to Por1 and markers for Complex III (Rip1), and for Complex IV (Cox2).

zinc concentration is below 200 μM. Detoxification of zinc within the vacuole is efficient and mutations that disrupt vacuolar zinc storage render cells very sensitive to zinc toxicity. Thus, the mitochondrial zinc pool is not likely to be a significant mechanism of zinc detoxification.

The matrix Zn(II) pool appears important in mitochondrial zinc metallation reactions. The plethora of Zn metalloenzymes within mitochondria implies that a significant bioavailable Zn(II) pool must exist for the metallation of these molecules upon their import. In support of this postulate is the observation that attenuation in the labile pool by the matrix-targeted m-Adh1 correlates with impaired oxidative phosphorylation and respiratory growth. The dominant negative effects of m-Adh1 do not arise from perturbation in metabolism within the matrix due to the catalytic activity of Adh1, because the same effects are observed with a catalytically inactive matrix Adh1. This suggests that Zn(II)-chelation is the likely cause of the respiration defect. This is corroborated by two observations. First, the respiratory growth of cells harboring m-Adh1 are partially rescued in by supplemental zinc in the growth medium, and second that m-Adh1 provokes respiratory deficiency in cells lacking the zinc importer, Zrt1. The dominant negative effects of m-Adh1 are not observed in cells propagated on zinc-sufficient standard culture medium. Under these culture conditions the presence of m-Adh1 results in an expansion of mitochondrial Zn(II) corresponding to formation of Zn-Adh1 and likely represents homeostatic regulation of the labile zinc pool.

Metal ion transporters in the mitochondrial IM have been identified for only Fe(II) ions. Transporters that mediate mitochondrial import of Zn(II), Mn(II), and Cu(I)/Cu(II) have not been defined. In an attempt to identify proteins important for mitochondrial import of Zn(II) or maintenance of the labile Zn(II) pool, we conducted two different high throughput screens. With a collection of yeast deletion strains of mitochondrial proteins, we screened for respiratory growth defects on Zn-limiting medium and identified *mzm1*Δ cells as sensitive to Zn limitation.

Mzm1 is a mitochondrial matrix protein that not only influences the matrix cationic Zn pool but also has a role in the assembly or stability of the bc_1 complex. Cells lacking Mzm1 exhibited respiratory growth sensitivity to both Zn-limited

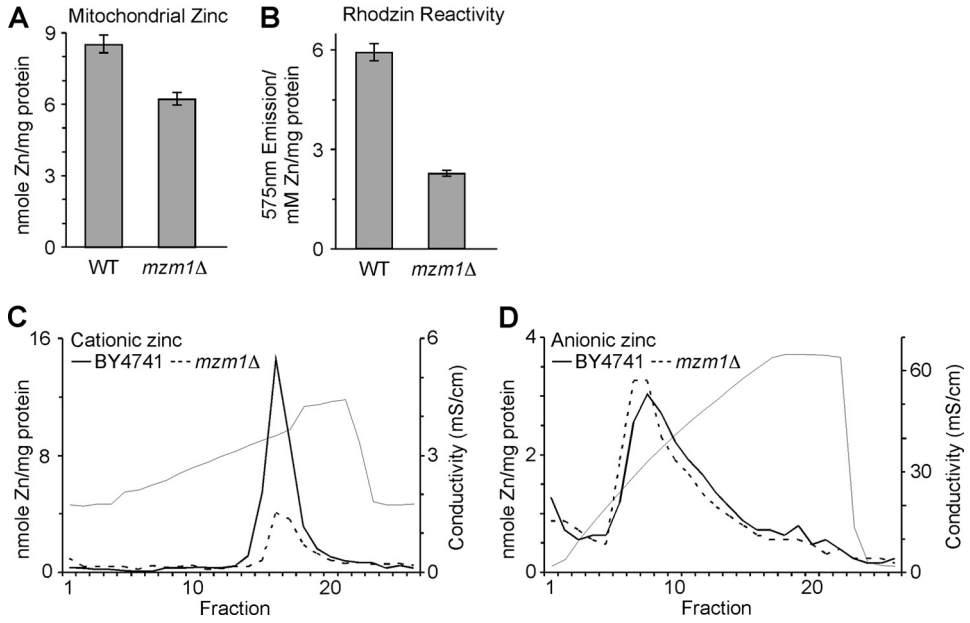

FIGURE 6. **Mitochondrial Zn defect in mzm1Δ cells.** Mitochondria were isolated for both WT and *mzm1*Δ from cells grown in yeast peptone 1% dextrose. *Panel A*, metal analysis of mitochondria (200 μg; $n = 3$). *Panel B*, mitochondria (50 μg) were sonicated in 0.1 ml 10 mM Tris, and the clarified lysate incubated with Rhodzin-3 to asses Zn-dependent fluorescence. Following fluorescent measurements, lysates were analyzed for metal content by ICP-OES ($n = 3$). *Panel C*, MonoS fractionation of *mzm1*Δ soluble mitochondrial lysate. *Panel D*, MonoQ fractionation of *mzm1*Δ soluble mitochondrial lysate.

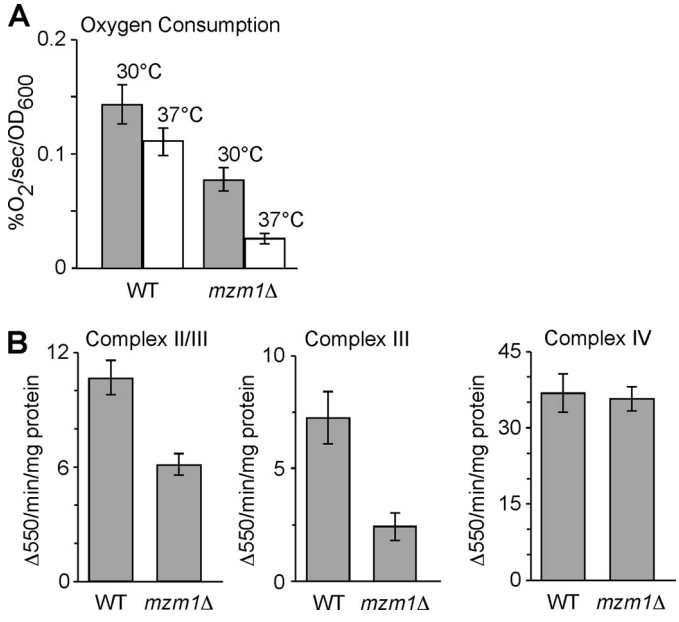

FIGURE 7. **Respiratory defect in *mzm1*Δ cells.** *Panel A*, total oxygen consumption of *mzm1*Δ relative to wild type at 30° and 37 °C. *Panel B*, analysis of succinate cytochrome *c* reductase activity (Complex II/III), ubiquinol cytochrome *c* reductase activity (Complex III), and cytochrome *c* oxidase activity (Complex IV) using 10–20 μg of mitochondria per reaction (see "Materials and Methods" for details) ($n = 3$ per assay).

medium and the presence of m-Adh1. The matrix cationic Zn(II) component was attenuated in *mzm1*Δ cells in both W303 and BY4741 backgrounds as seen by MonoS chromatography and RhodZin-3 reactivity. In addition, *mzm1*Δ cells have decreased accumulation of the dimeric bc_1 complex. Reintroduction of the *MZM1* gene into the mutant cells suppressed both the mitochondrial zinc defect and the Complex III deficiency suggesting a link between the two phenotypes. However, supplemental zinc did not restore bc_1 complex activity in the mutant cells. This is consistent with the failure of supplemental zinc to fully restore glycerol growth of the mutant at 37 °C. Thus, Mzm1 may have other roles and may affect zinc homeostasis indirectly.

The nature of the link between zinc and the bc_1 complex is not obvious as none of the bc_1 complex subunits have known Zn-binding proteins. However, the matrix-facing Cor1 and Cor2 bc_1 subunits are homologous to the MPP zinc-metalloproteinase (26, 27). MPP is a dimeric proteinase with an HxxEH Zn motif in one subunit. The core complex in the potato bc_1 complex functions as the general MPP in that species (28). However, vertebrate bc_1 core subunits have an altered motif with a tyrosine replacing one His residue (26). The yeast Cor1 and Cor2 bc_1 complex subunits lack the H*XX*EH motif, so it is unlikely that a MPP-like function is conserved. A second link between zinc and the bc_1 complex is that the respiratory complex is inhibited by Zn(II) and two Zn(II) binding sites per monomer were mapped in the avian complex (27). The two sites are spatially close to ubiquinone binding site.

Two other scenarios are envisioned for the observed zinc/bc_1 relationship. First, Mzm1 may have two distinct roles in the maintenance of the matrix Zn pools and assembly/stability of the bc_1 complex. Alternatively, the assembled bc_1 complex may have a role in mitochondrial Zn import or efflux such that cells impaired in bc_1 formation may be compromised in mitochondrial zinc. A related link between a respiratory complex and mitochondrial metal pools was observed with *coa1*Δ and *shy1*Δ cells. Both mutants are impaired in the biogenesis of cytochrome *c* oxidase and in the maintenance of the matrix bioavailable Cu(I) pool (20, 29). Coa1 and Shy1 form complexes with newly synthesized Cox1 during its maturation and we postulated that these assembly intermediates may also modulate import of Cu(I) across the IM. Whereas *coa1*Δ and *shy1*Δ cells are weakly suppressed by supplemental copper in cultures, the respiratory defect of *mzm1*Δ cells is not suppressed by supplemental zinc. Future studies will focus on the role of Mzm1 in bc_1 complex biogenesis as well as matrix zinc maintenance.

The second screen was with the same collection of mutant strains transformed with a vector expressing matrix-targeted m-Adh1. Seven deletion mutants were observed to exhibit a respiratory growth deficiency in the presence of m-Adh1 but not cytosolic c-Adh1. Although total mitochondrial zinc was not markedly attenuated in most of these strains, RhodZin-3 reactivity of purified mitochondria was attenuated in several:

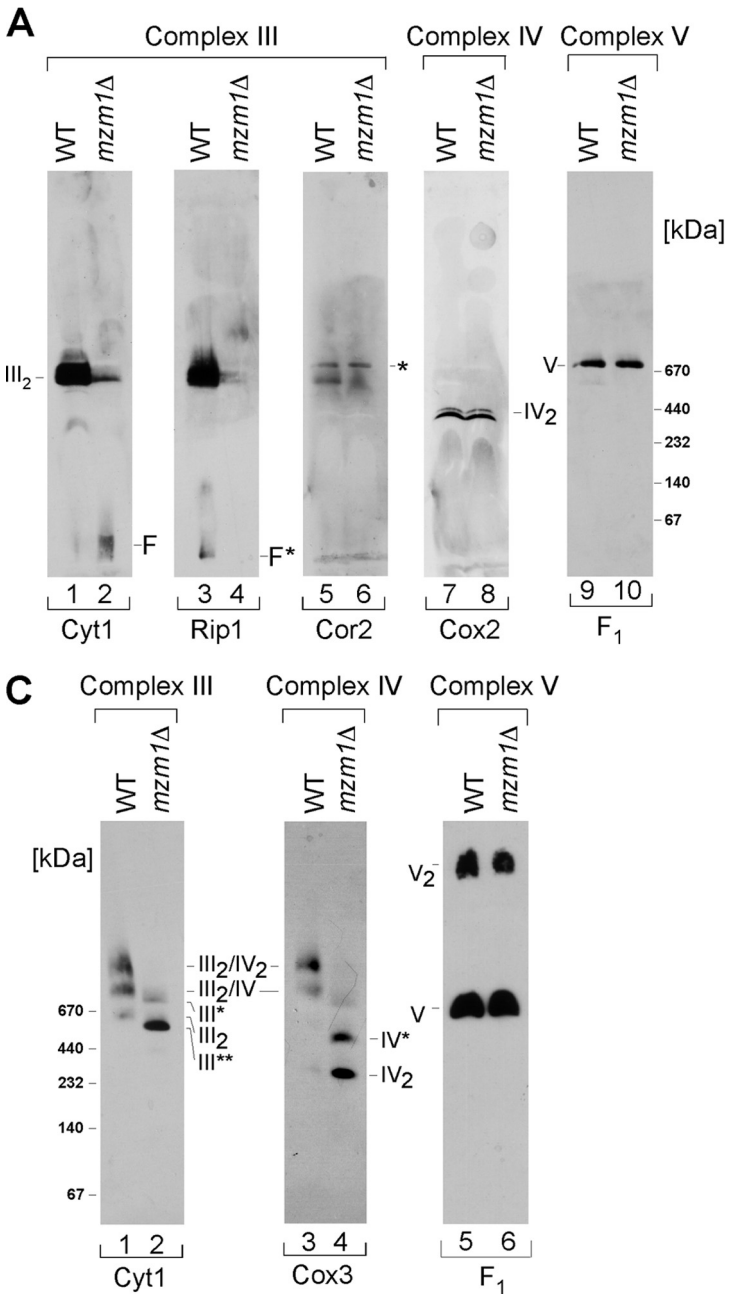

FIGURE 8. **The bc_1 complex is impaired in *mzm1*Δ cells.** *Panel A*, mitochondria (75 μg) were solubilized in buffer containing 1% dodecyl-β-D-maltoside (*DDM*) and analyzed by BN-PAGE. Detection with Cyt1 (cytochrome c_1, *lanes 1* and *2*), Rip1 (Rieske Iron-sulfur Protein 1, *lanes 3* and *4*), and Cor2 (core protein 2, *lanes 5* and *6*) reveal the state of dimeric Complex III (III_2) in both WT and *mzm1*Δ. Detection of either Cox2 (*lanes 7* and *8*) or F_1 (*lanes 9* and *10*) representing Complex IV and V, respectively, shows no defects between *mzm1*Δ and WT cells. Low molecular weight or free Cyt1 (*F*); low molecular weight or free Rip1 (*F**); residual Complex V signal (*). *Panel B*, immunoblot analysis of wild-type and *mzm1*Δ cells for protein levels of Complex III subunits Rip1, Cyt1, and Cor2 as well as Cox2 (Complex IV) and porin. *Panel C*, mitochondria (150 μg) solubilized in buffer containing 1% digitonin were fractionated on a continuous 5–13% gradient gel and protein analyzed by BN-PAGE. Detection with the Complex III subunit Cyt1 reveals subassembly complexes (III*, and III**) together with dimeric Complex III (III_2) and the higher Complex III/IV supercomplexes (III_2/IV, and III_2/IV_2). Detection with the Complex IV component, Cox3, also reveals a Complex IV intermediate (IV*) in addition to dimeric Complex IV (IV_2). Detection with the Complex V subunit, F1, reveals no defect between *mzm1*Δ and wild type.

natively, Mdh1 was recently shown to associate with submicromolar affinity with the bc_1 complex via the matrix-facing Cor1 and Cor2 subunits (30). This interaction was shown to stimulate the bc_1 activity and enhance the reverse Mdh1 reaction thereby consuming oxaloacetate. Cells lacking Mdh1 were found to be only modestly impaired in bc_1 activity (~83% of wild type), so the link of Zn and bc_1 assembly remains unclear. Nfu1 is one of three matrix scaffold proteins for the assembly of Fe/S clusters. Mis1 is a mitochondrial candidate C1-tetrahydrofolate synthase (31). One-carbon transfer reactions are mediated by tetrahydrofolate and derivatives of THF are required for the biosynthesis of purines, thymidylate, pantothenate, and certain amino acids. C1-tetrahydrofolate synthases mediate interconversion of different oxidation states of THF derivatives. Cells lacking the cytosolic Ade3 C1-tetrahydrofolate synthase exhibit auxotrophies for adenine and histidine, whereas cells lacking the mitochondrial Mis1 C1-tetrahydrofolate synthase lack an obvious effect on adenine or histidine biosynthesis or respiration (31). Thus, Mis1 and Ade3 have distinct functions and the physiological significance of the mitochondrial Mis1 remains unclear. Although Msb1 is a mitochondrial protein, it is implicated in glucan synthesis and the Pkc1-MAPK pathway (32). No clear mitochondrial function is known for Msb1. No function is ascribed for Tbs1 either. None of these molecules appear to be candidates for membrane Zn(II) transporters. The identity of the mitochondrial Zn(II) transporter(s) remains unresolved. No transporter-encoding genes were identified in our screens suggesting that mitochondrial zinc transporters are either essential, and therefore would not be included among the strains tested, or redundant with other genes such that loss of one does not greatly alter mitochondrial zinc homeostasis.

Mzm1, Cit1, Mdh1, Nfu1, Mis1, Msb1, and Tbs1 were all found to contribute to the maintenance of the labile cationic Zn(II) pool. Cit1 and Mdh1 are citric acid cycle enzymes, so the depletion of these molecules will alter the levels of matrix metabolites that may contribute to the cationic Zn(II)-component. Alter-

Acknowledgments—We thank Dr. Amanda Bird for her gift of the Adh1 expression construct and Dr. Jared Rutter for participation in

the CEMH yeast consortium efforts. We acknowledge the support of the Center for Excellence in Molecular Hematology (CEMH) core facility for FPLC chromatography and pilot project funding (DK P30 072437).

REFERENCES

1. Atkinson, A., and Winge, D. R. (2009) *Chem. Rev.* **109,** 4708–4721
2. Mesecke, N., Bihlmaier, K., Grumbt, B., Longen, S., Terziyska, N., Hell, K., and Herrmann, J. M. (2008) *EMBO Rep.* **9,** 1107–1113
3. Coyne, H. J., 3rd, Ciofi-Baffoni, S., Banci, L., Bertini, I., Zhang, L., George, G. N., and Winge, D. R. (2007) *J. Biol. Chem.* **282,** 8926–8934
4. Eide, D. J. (2006) *Biochim. Biophys. Acta* **1763,** 711–722
5. Jackson, K. A., Helston, R. M., McKay, J. A., O'Neill, E. D., Mathers, J. C., and Ford, D. (2007) *J. Biol. Chem.* **282,** 10423–10431
6. Cousins, R. J., Liuzzi, J. P., and Lichten, L. A. (2006) *J. Biol. Chem.* **281,** 24085–24089
7. Thompson, R. B., Peterson, D., Mahoney, W., Cramer, M., Maliwal, B. P., Suh, S. W., Frederickson, C., Fierke, C., and Herman, P. (2002) *J. Neurosci. Methods* **118,** 63–75
8. Domaille, D. W., Que, E. L., and Chang, C. J. (2008) *Nat. Chem. Biol.* **4,** 168–175
9. Haase, H., and Beyersmann, D. (2002) *Biochem. Biophys. Res. Commun.* **296,** 923–928
10. Frederickson, C. J. (1989) *Int. Rev. Neurobiol.* **31,** 145–238
11. Palmiter, R. D., Cole, T. B., Quaife, C. J., and Findley, S. D. (1996) *Proc. Natl. Acad. Sci. U.S.A.* **93,** 14934–14939
12. Linkous, D. H., Flinn, J. M., Koh, J. Y., Lanzirotti, A., Bertsch, P. M., Jones, B. F., Giblin, L. J., and Frederickson, C. J. (2008) *J. Histochem. Cytochem.* **56,** 3–6
13. Sensi, S. L., Ton-That, D., Weiss, J. H., Rothe, A., and Gee, K. R. (2003) *Cell Calcium* **34,** 281–284
14. Sensi, S. L., Ton-That, D., Sullivan, P. G., Jonas, E. A., Gee, K. R., Kaczmarek, L. K., and Weiss, J. H. (2003) *Proc. Natl. Acad. Sci. U.S.A.* **100,** 6157–6162
15. Leskovac, V., Trivić, S., and Pericin, D. (2002) *FEMS Yeast Res.* **2,** 481–494
16. Diekert, K., De Kroon, A. I., Kispal, G., and Lill, R. (2001) *Methods Cell Biol.* **65,** 37–51
17. Wittig, I., Braun, H. P., and Schägger, H. (2006) *Nat. Protoc.* **1,** 418–428
18. Capaldi, R. A., Marusich, M. F., and Taanman, J. W. (1995) *Methods Enzymol.* **260,** 117–132
19. Cobine, P. A., Ojeda, L. D., Rigby, K. M., and Winge, D. R. (2004) *J. Biol. Chem.* **279,** 14447–14455
20. Cobine, P. A., Pierrel, F., Bestwick, M. L., and Winge, D. R. (2006) *J. Biol. Chem.* **281,** 36552–36559
21. Hess, D. C., Myers, C. L., Huttenhower, C., Hibbs, M. A., Hayes, A. P., Paw, J., Clore, J. J., Mendoza, R. M., Luis, B. S., Nislow, C., Giaever, G., Costanzo, M., Troyanskaya, O. G., and Caudy, A. A. (2009) *PLoS Genet.* **5,** e1000407
22. Dinur-Mills, M., Tal, M., and Pines, O. (2008) *PLoS ONE* **3,** e2161
23. White, C., and Gadd, G. M. (1987) *J. Gen. Microbiol.* **133,** 727–737
24. MacDiarmid, C. W., Gaither, L. A., and Eide, D. (2000) *EMBO J.* **19,** 2845–2855
25. Simm, C., Lahner, B., Salt, D., LeFurgey, A., Ingram, P., Yandell, B., and Eide, D. J. (2007) *Euk. Cell* **6,** 1166–1177
26. Iwata, S., Lee, J. W., Okada, K., Lee, J. K., Iwata, M., Rasmussen, B., Link, T. A., Ramaswamy, S., and Jap, B. K. (1998) *Science* **281,** 64–71
27. Berry, E. A., Zhang, Z., Bellamy, H. D., and Huang, L. (2000) *Biochim. Biophys. Acta* **1459,** 440–448
28. Braun, H. P., Emmermann, M., Kruft, V., and Schmitz, U. K. (1992) *EMBO J.* **11,** 3219–3227
29. Pierrel, F., Bestwick, M. L., Cobine, P. A., Khalimonchuk, O., Cricco, J. A., and Winge, D. R. (2007) *EMBO J.* **26,** 4335–4346
30. Wang, Q., Yu, L., and Yu, C. A. (2010) *J. Biol. Chem.*, **285,** 10408–10414
31. Shannon, K. W., and Rabinowitz, J. C. (1988) *J. Biol. Chem.* **263,** 7717–7725
32. Sekiya-Kawasaki, M., Abe, M., Saka, A., Watanabe, D., Kono, K., Minemura-Asakawa, M., Ishihara, S., Watanabe, T., and Ohya, Y. (2002) *Genetics* **162,** 663–676